# Subversion of CtBP1-controlled macropinocytosis by human adenovirus serotype 3

**Beat Amstutz[1], Michele Gastaldelli[1], Stefan Kälin[1], Nicola Imelli[1], Karin Boucke[1], Eliane Wandeler[1], Jason Mercer[2], Silvio Hemmi[3] and Urs F Greber[1],***

[1]Institute of Zoology, University of Zürich, Zürich, Switzerland, [2]Institute of Biochemistry, ETH Zürich, Zürich, Switzerland and [3]Institute of Molecular Biology, University of Zürich, Zürich, Switzerland

Endocytosis supports cell communication, growth, and pathogen infection. The species B human adenovirus serotype 3 (Ad3) is associated with epidemic conjunctivitis, and fatal respiratory and systemic disease. Here we show that Ad3 uses dynamin-independent endocytosis for rapid infectious entry into epithelial and haematopoietic cells. Unlike Ad5, which uses dynamin-dependent endocytosis, Ad3 endocytosis spatially and temporally coincided with enhanced fluid-phase uptake. It was sensitive to macropinocytosis inhibitors targeting F-actin, protein kinase C, the sodium–proton exchanger, and Rac1 but not Cdc42. Infectious Ad3 macropinocytosis required viral activation of p21-activated kinase 1 (PAK1) and the C-terminal binding protein 1 of E1A (CtBP1), recruited to macropinosomes. These macropinosomes also contained the Ad3 receptors CD46 and αv integrins. CtBP1 is a phosphorylation target of PAK1, and is bifunctionally involved in membrane traffic and transcriptional repression of cell cycle, cancer, and innate immunity pathways. Phosphorylation-defective S147A-CtBP1 blocked Ad3 but not Ad5 infection, providing a direct link between PAK1 and CtBP1. The data show that viruses induce macropinocytosis for infectious entry, a pathway used in antigen presentation and cell migration.

## Introduction

Animal cells support a variety of endocytic pathways to coordinate signal transduction, cell growth, differentiation,

*Corresponding author. Institute of Zoology, University of Zuerich, Winterthurerstrasse 190, CH-8057 Zurich, Switzerland.
Tel.: +41 44 635 4841; Fax: +41 44 635 6822;
E-mail: ufgreber@zool.unizh.ch

death, and also pathogen infection (Marsh and Helenius, 2006). Besides clathrin-mediated endocytosis, dynamin-dependent endocytic pathways include phagocytosis, the interleukin-2 receptor and intercellular adhesion molecule 1 routes, caveolar and lipid raft-dependent uptake, or dorsal ruffling leading to WAVE complex-dependent endocytosis (Gruenberg and van der Goot, 2006; Marsh and Helenius, 2006; Orth et al, 2006). Only a few dynamin-independent pathways are known, for example, cholera toxin uptake by means of the glycosylphosphatidylinositol (GPI)-anchored protein pathway (Kirkham et al, 2005), or macropinocytosis, which engulfs large plasma membrane domains into spherical endosomes (Schnatwinkel et al, 2004). Macropinocytosis can be induced by growth factors, Ras, or Src tyrosine kinase. It clears bacterial infections, removes apoptotic bodies, and is an important element of innate immunity and cell migration (Wu et al, 2006). Constitutive macropinocytosis supports antigen processing and presentation in dendritic cells. In viral infections, macropinocytosis is an accessory pathway triggered by HIV (Marechal et al, 2001; Liu et al, 2002), and human adenovirus types 2 and 5 (Ad2/5) in respiratory epithelial cells (Meier et al, 2002). It has remained unclear, however, whether macropinocytosis is an infectious entry pathway for pathogens.

Adenoviruses are a diverse family of agents. They infect the upper and lower respiratory tracts and the urinary and digestive tracts, and give rise to epidemic conjunctivitis. The species B serotypes Ad3, Ad7, and Ad11 are associated with morbidity and mortality and with exacerbations of asthmatic conditions, and Ad3 has been associated with epidemic conjunctivitis (Hayashi and Hogg, 2007). The nature of the Ad3 receptor has been debated (Sirena et al, 2004; Marttila et al, 2005), but recent mutagenesis experiments have mapped the Ad3 binding site of CD46 to the distal consensus repeats 1 and 2 (Fleischli et al, 2007), in close agreement with the crystal structure of the Ad11 fibre knob on CD46 (Persson et al, 2007). CD46 protects autologous cells from complement attack and links innate and acquired immunity in macrophages and lymphocytes (Liszewski and Atkinson, 1996; Riley-Vargas et al, 2004). The extracellular domain contains partly overlapping binding sites for the complement factors C3b and C4b and for different viruses and bacteria. In T cells, ligand-induced crosslinking of CD46 stimulates the phosphorylation of Cbl and LAT and the activation of Vav, Rac, and the Erk1/2 MAP kinase pathway. The Rac1 GTPase orchestrates CD46 downregulation by macropinocytosis (Crimeen-Irwin et al, 2003) and increases immune suppression and susceptibility to complement-mediated lysis (Kemper et al, 2005).

Here, we show that infectious endocytic uptake of Ad3 occurs through macropinocytosis. It is controlled by a transcriptional corepressor, the C-terminal binding protein 1 of E1A (CtBP1). CtBP1 occurs in two spliced forms, long and short (CtBP1-L/S). CtBP1-S (also called brefeldin A adenosine

diphosphate ribosylated substrate) lacks 11 N-terminal amino acids, and like CtBP1-L is involved in dynamin-independent endocytosis (Chinnadurai, 2002; Bonazzi et al, 2005). It is observed at Golgi membranes and functions in mitotic partitioning of the Golgi apparatus and membrane trafficking (Colanzi et al, 2007). It is also found on dense bodies of synaptic termini where it may have a tethering role in membrane organization (Gallop et al, 2005; tom Dieck et al, 2005). The two mammalian CtBP genes 1 and 2 have partly overlapping transcriptional functions in tumorigenesis, apoptosis, development, cell differentiation, cell cycle regulation, and viral infection (Berk, 2005). In normal cells, CtBP1 heterodimerizes with CtBP2 and shuttles between the nucleus and the cytoplasm depending on post-translational modifications and binding to PDZ proteins (Barnes et al,

2003; Verger et al, 2006). Here, we address a cytoplasmic function of CtBP1 in infectious macropinocytic uptake of Ad3.

## Results

### αv integrins in dynamin-dependent and dynamin-independent Ad3 endocytosis

Integrins have been known to support infectious endocytosis of species C human adenoviruses, such as respiratory Ad2 and Ad5 (Stewart and Nemerow, 2007). We tested whether Ad3 infection required αv integrins. Ad3-eGFP transduction of αv integrin-deficient, CD46-positive M21L melanoma cells was reduced compared to αv integrin-positive M21 cells, although binding was not affected (Figure 1A and B), in agreement with earlier reports on infection (Mathias et al,
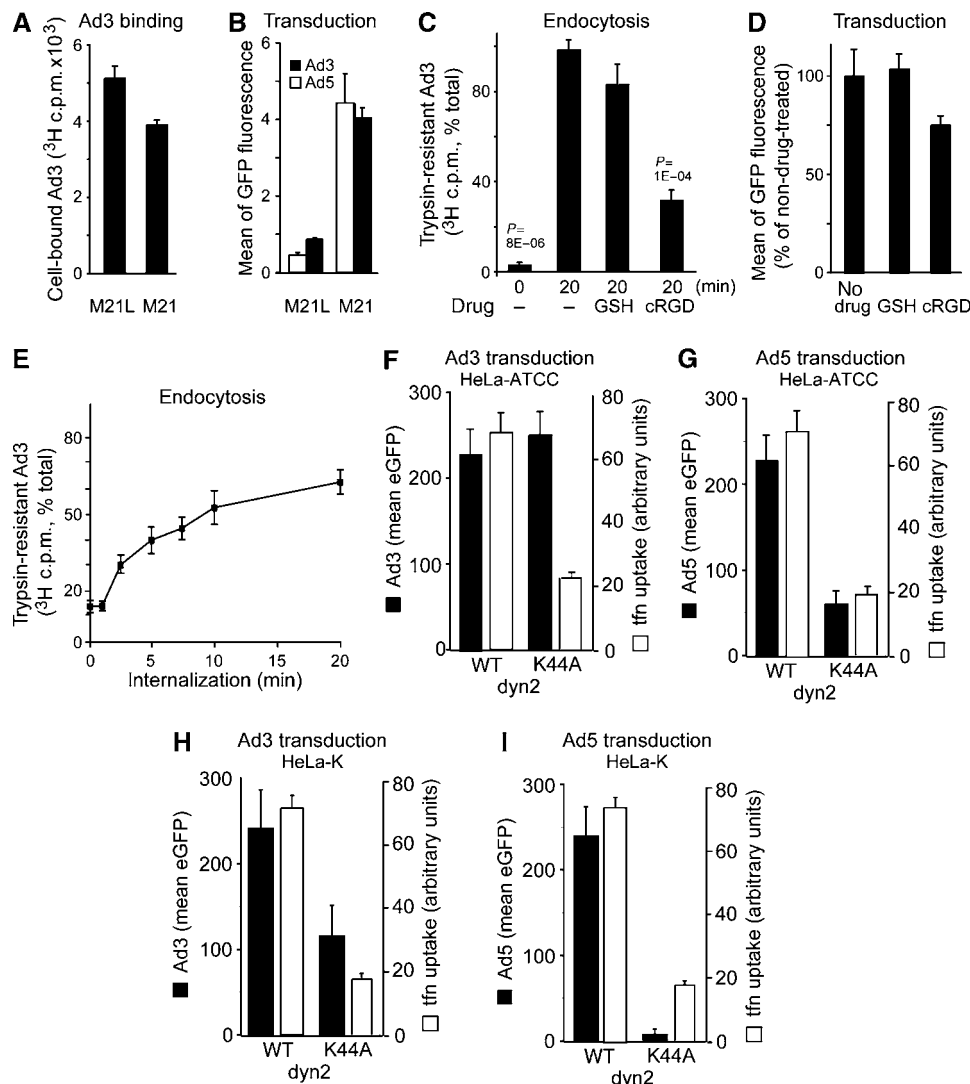


**Figure 1** Infectious Ad3 endocytosis of HeLa cells requires αv integrins and to a low extent dynamin. (**A**) Human melanoma M21 or M21L cells were incubated with [³H]thymidine-labelled Ad3 in the cold and analysed for cell-associated radioactivity ($10^6$ cells, 0.75 μg Ad3). (**B**) M21 or M21L cells were transduced with Ad3-eGFP or Ad5-eGFP (MOI 5) and analysed by flow cytometry 8 h p.i. (**C, D**) [³H]thymidine-labelled Ad3 ($8 \times 10^5$/ml; 50 000 c.p.m.) was cold bound to HeLa-ATCC cells (2000 c.p.m. bound) and warmed for 0 or 20 min in the presence or absence of glutathione (GSH) or cyclic RGD peptide (cRGD, 0.2 mM), trypsinized in the cold, and analysed for cell-associated (internalized) or released [³H]thymidine-labelled Ad3 by liquid scintillation counting. Cells were treated with GSH or cRGD, infected with Ad3-eGFP (MOI 5), and analysed for GFP expression by flow cytometry 6 h p.i. (**E**) Kinetics of Ad3 endocytosis measured by trypsin resistance as described in panel C (100% equivalent to 2000 c.p.m.). Means of triplicate dishes of one representative experiment are shown (A–E). (**F–I**) Ad3-eGFP and Ad5-eGFP transduction (6 h) and transferrin–Alexa647 internalization (10 μg/ml transferrin in the last 30 min of infection, open bars) in HeLa-ATCC or HeLa-K cells transfected with WT dyn2 or K44A dyn2 for 48 h. Single-cell analysis by confocal microscopy (MOI 5), showing the mean of at least 40 blindly selected cells, is shown. One representative experiment is shown (F–I).
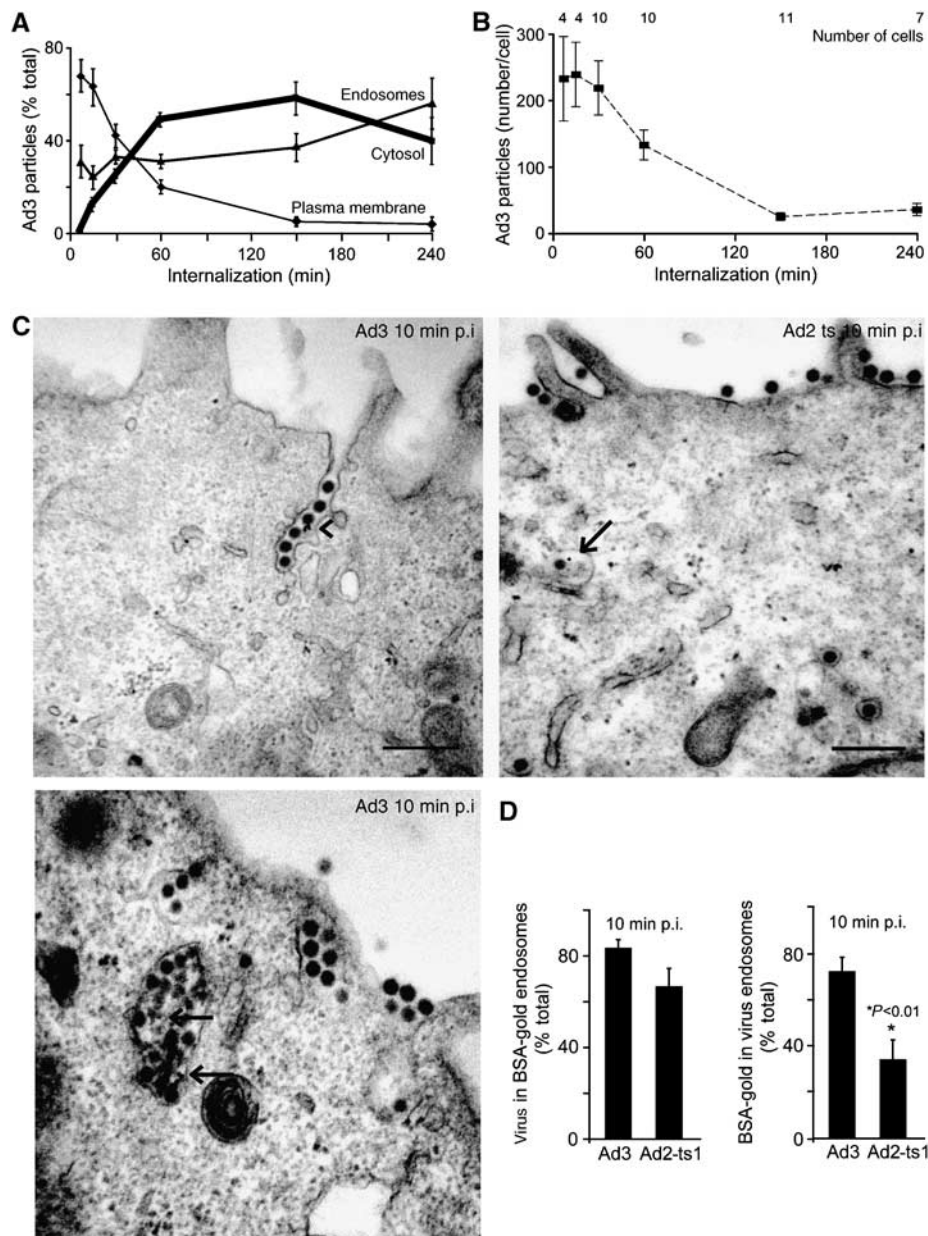
**Figure 2** Quantitative EM analyses of Ad3 endocytosis and endosomal escape. (**A**) Distribution of cold-bound Ad3 ($5 \times 10^5$ viral particles per cell, $4^\circ$C, 60 min) on the plasma membrane, endosomes, and the cytosol (bold line) upon internalization at $37^\circ$C. (**B**) Analyses of the total number of particles and cells. (**C, D**) Enrichment of Ad3 in fluid-phase-positive endosomes. HeLa cells were incubated with Ad3 or Ad2-ts1 in the cold (MOI as in (A)), washed, pulsed with BSA-gold for 10 min, fixed for ultrathin-section EM analyses, and quantified for viral particles in either gold-positive endosomes (arrows) or gold particles in endosomes that contain Ad3 or Ad2-ts1, respectively. Viruses in plasma membrane invaginations are indicated by an arrowhead.

1994). Similar results were obtained with Ad5 (Figure 1B). Soluble RGD peptides inhibited both Ad3 endocytosis measured by trypsin resistance of [³H]thymidine-labelled virions (Figure 1C) and transduction of Ad3-eGFP (Figure 1D). Quantitative internalization assays at low multiplicity of infection (MOI, 5 infectious particles bound per cell) indicated that more than 50% of the surface-bound virions were internalized within 20 min (Figure 1E), consistent with virus uptake measurements at high MOI (Figure 2A). This result was similar for Ad2 (Greber *et al*, 1993) and the Ad3-related Ad7 (Miyazawa *et al*, 1999). Ad3-eGFP transduction of HeLa-ATCC cells was not sensitive to dominant-negative (dn) K44A dynamin2 (dyn2), which blocked transferrin uptake, whereas

Ad5 was strongly inhibited by K44A-dyn2 (Figure 1F and G). In HeLa-K cells (a variant of HeLa-ATCC), K44A-dyn2 inhibited both Ad3- and Ad5-mediated eGFP transduction, although Ad5 was affected more strongly, and transferrin uptake was inhibited similar to that in HeLa-ATCC cells (Figure 1H and I). To further assess an involvement of dynamin-mediated endocytosis in Ad3 infection, we expressed dn constructs of amphiphysin and Eps15 and measured nuclear targeting of fluorescent Ad3 (Nakano and Greber, 2000). The D36R mutant of the amphiphysin2 SH3 domain, which tightly binds to and prevents self-assembly of dynamin (Owen *et al*, 1998), and the Eps15 EH29 mutant lacking EH domain 2 but retaining binding to the adaptor

complex 2 (Benmerah *et al*, 1999) blocked transferrin uptake but not Ad3 nuclear targeting, indicating that dynamin and Eps15 were not involved in Ad3 endocytosis in HeLa-ATCC (Supplementary Figure 1). This suggested a cell type-dependent, but low-level involvement of dynamin in Ad3 infection and confirms a strong dynamin requirement for Ad5 infection.

### Macropinocytosis is an infectious entry route of Ad3

Electron microscopy (EM) analyses of incoming Ad3 at high MOI of 5000 confirmed that the bulk of Ad3 was internalized rapidly and efficiently (Figure 2A). Viral escape to the cytosol occurred with a half-time of 30–40 min post infection (p.i.). At 150 min p.i., 90% of the particles morphologically disappeared, indicating capsid disassembly and/or degradation (Figure 2B). Ad3 particles were frequently found in smooth invaginations of the plasma membrane and large vesicles with multiple virus particles (Figure 2C, 10 min p.i.). The limiting membrane of viral vesicles was not stained with cell-impermeable cationized ferritin added after virus internalization, indicating that these structures were in the cytosol (data not shown). About 80% of the Ad3-carrying vesicles contained fluid-phase BSA-gold, similar to vesicles with Ad2-ts1 (Figure 2D). Ad2-ts1 was internalized in the absence of macropinocytosis with similar kinetics as wild-type (WT) Ad2 (Meier *et al*, 2002). In contrast to Ad2-ts1, Ad3 endosomes contained more BSA-gold, demonstrating that Ad3 enters along a pathway rich in fluid phase (Figure 2D). Dextran measurements confirmed that Ad3 stimulated fluid uptake (Figure 3A and B). Ad3- but not Ad2-stimulated dextran uptake was completely abolished in the presence of excess Ad3 fibre knob protein, which binds CD46 and blocks cell attachment of Ad3 (Sirena *et al*, 2004) (Figure 3C). The fibre knob of the Ad3-related Ad11 is a trimer that binds three soluble CD46 extracellular consensus repeats (Persson *et al*, 2007). The data thus suggested that multiple fibres or additional capsid components of the Ad3 particle are required to trigger CD46-mediated macropinocytosis.

To test whether antibody-mediated CD46 crosslinking triggered fluid-phase uptake, HeLa-ATCC cells were incubated with the monoclonal anti-CD46 IgG antibody E4-3, followed by anti-IgG crosslinking antibodies. Under these conditions, we measured a modest but significant 1.6-fold increase of dextran uptake compared to control cells or cells incubated with 5× lower concentrations of E4-3 (Figure 3D). This was in agreement with an earlier study reporting that low antibody crosslinking of CD46 leads to CD46 internalization by constitutive clathrin-mediated endocytosis, whereas a high degree of crosslinking leads to cell-surface ruffling and macropinocytosis (Crimeen-Irwin *et al*, 2003). Cells incubated with the anti-αv integrin antibody LM609 but not the function-blocking P1F6 stimulated dextran uptake 1.5-fold (Figure 3D). The combination of E4.3 and LM609 gave a robust two-fold stimulation of dextran uptake, suggesting that simultaneous CD46 and αv integrin crosslinking potentiates fluid-phase uptake. Ad3 alone was more potent than antibodies or the phorbol ester PMA, and depended on soluble cyclic RGD (arginine–glycine–aspartate) peptides (Figure 3D and E). We concluded that Ad3 stimulates fluid-phase uptake by the combined ligation of CD46 and αv integrins.

Next, we assessed Ad3-stimulated dextran uptake by pharmacological inhibitors. Ad3-stimulated dextran uptake was sensitive to cytochalasin D and jasplakinolide, which depolymerize and stabilize F-actin, respectively, and the protein kinase C inhibitor Gö6976, which blocks the calcium-dependent PKC α and β isoforms but not calcium-independent PKCs (Gschwendt *et al*, 1996; Davies *et al*, 2000), and strongly blocked by the sodium/proton exchange inhibitor 5-(*N*-ethyl-*n*-isopropyl)-amiloride (EIPA) (Figure 3F and G). Importantly, all these classical macropinocytosis inhibitors significantly reduced Ad3 infection, although jasplakinolide could also have post-endocytic effects inhibiting Ad3-eGFP expression, as concluded by the late addition of the drug (Figure 3H). These inhibitors as well as the Rho GTPase inhibitor toxin B prevented viral endocytosis measured at low MOI using the trypsin assay (Figure 4A). The analysis of subcellular localization of Ad3 particles at the plasma membrane, endosomes, and the cytosol using quantitative thin-section EM at high MOI confirmed these results (Figure 4B and Supplementary Figure 2). Interestingly, both Ad3-stimulated dextran uptake and infection were also inhibited in cells depleted of clathrin heavy chain (CHC; Figure 4C and D). Infection of CHC-depleted cells with SV-40, which enters by clathrin-independent endocytosis (Marsh and Helenius, 2006), was not affected (data not shown). Importantly, CHC depletion did not affect the expression of CD46, coxsackievirus adenovirus receptor (CAR), or αv integrins on the cell surface (data not shown). It also did not affect basal dextran uptake, which occurs by clathrin-dependent and clathrin-independent endocytosis, but blocked transferrin internalization (data not shown). This could suggest that another endocytic process that is different from viral macropinocytosis could compensate for the loss of clathrin-mediated endocytosis, as previously suggested for dynamin-inhibited cells, which upregulate an unknown dynamin-independent pathway (Damke *et al*, 1994). Importantly, most of the Ad3 particles were found in large endocytic vesicles and only a minor fraction was found in clathrin-coated invaginations or vesicles (less than 1%; for representative EM images, see Supplementary Figure 3), suggesting that clathrin has a minor role in Ad3 endocytosis. This was confirmed by siRNA knockdown of CHC and quantitative EM analyses showing that CHC knockdown reduced cytosolic Ad3 but not plasma membrane or endosomal Ad3 (Figure 4E). This shows that at high MOI, Ad3 can internalize by a clathrin-independent mechanism in the absence of fluid-phase stimulation. It is likely that clathrin is required for endosomal escape of Ad3 and facilitates dextran uptake, possibly involving cytoplasmic membrane transport processes, such as retromer-mediated sorting from endosomes to the Golgi (Popoff *et al*, 2007).

### Infectious Ad3 macropinocytosis requires PAK1 activation and CtBP1

Dynamin-independent endocytosis of GPI-anchored proteins into early endosomal antigen 1-positive endosomes can occur along the GEEC pathway (GPI-anchored proteins-enriched early endosomal compartment) involving Cdc42 (Mayor and Pagano, 2007). The expression of the dn T17N–Cdc42 had no effect on Ad3 transduction, whereas dn T17N–Rac1 blocked Ad3-eGFP expression (Figure 5A and Supplementary Figure 4) and dextran uptake (data not shown), consistent
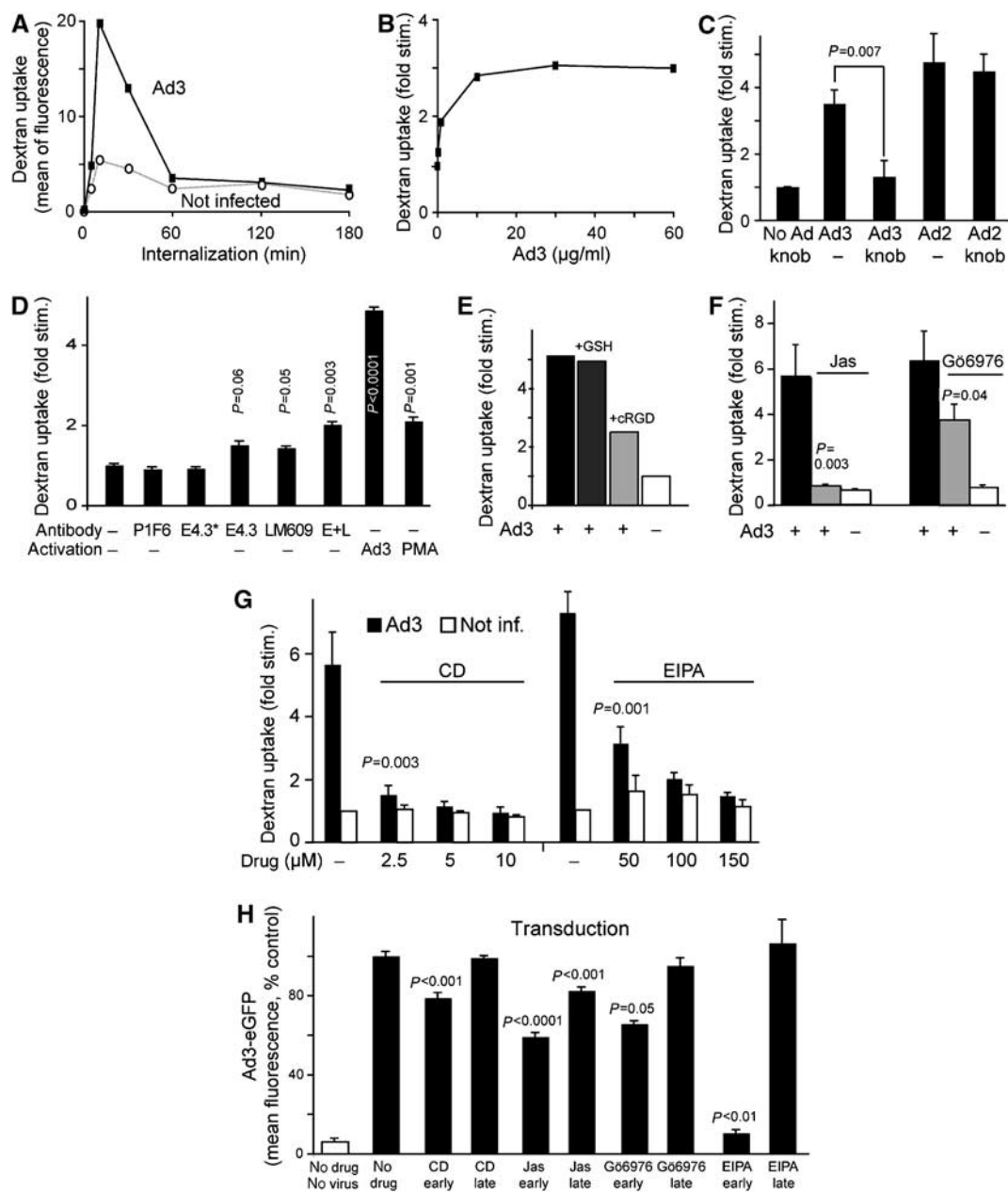
**Figure 3** CD46-, integrin-, F-actin-, PKC-, and EIPA-dependent stimulation of fluid-phase endocytosis by Ad3. (**A**) Ad3 transiently stimulates dextran uptake. HeLa-ATCC cells were incubated with Ad3 (5 μg/ml, equivalent to 2000 particles bound per cell) in the cold for 60 min, or noninfected, warmed for 0, 5, 30, 60, 120, or 180 min, pulsed with dextran—FITC, and analysed by flow cytometry as described in Materials and methods. One out of three representative experiments is shown. (**B**) Dose dependence of fluid-phase uptake stimulation expressed as fold stimulation over noninfected cells. HeLa cells were incubated with different amounts of Ad3 (0, 0.5, 1, 10, 30, and 60 μg/ml) in the cold, warmed for 5 min, pulsed with dextran–FITC for 5 min, washed, and analysed by flow cytometry. One out of two similar experiments is shown. (**C**) Specificity of Ad3-stimulated fluid-phase endocytosis. HeLa cells were incubated with Ad3 or Ad2 (5 μg/ml) in the presence or absence of Ad3 fibre knob (5 μg/ml) and analysed for dextran–FITC stimulation as described above. (**D**) Fluid-phase stimulation by anti-CD46 and anti-integrin antibodies. HeLa cells were incubated with 4 μg/ml anti-CD46 antibody E4.3, or 0.8 μg/ml E4.3 (E4.3*), anti-αv β5 integrin (P1F6), anti-αv β3 (LM609), or a combination of E4.3 plus LM609 (E + L, 4 μg/ml each) in cold RPMI medium for 1 h, washed, and incubated with goat anti-mouse IgG antibodies (10 μg/ml), Ad3, or the phorbol ester PMA (Meier *et al*, 2002) on ice for 30 min. They were then warmed in the presence of dextran–FITC for 10 min and analysed by flow cytometry. The experiment was performed in triplicate and repeated once. (**E–G**) Measurement of Ad3-induced dextran–FITC uptake 10 min p.i. in the presence or absence of cyclic RGD peptides (0.1 mM; Meier *et al*, 2002), jasplakinolide (Jas, 40 nM), the PKC inhibitor Gö6976 (1 μM), or different concentrations of cytochalasin D (CD) or EIPA. (**H**) Ad3-eGFP transduction (1000 viral particles/cell) of HeLa cells pretreated with CD, Jas, Gö6976, or EIPA. Gö6976 and EIPA were present during 1 h of warm infection and were then washed off (early), or present till 120–180 min p.i. (late), followed by flow cytometry of eGFP 6 h p.i. CD and Jas were present during the entire incubation time (early) or added 1 h after warming (late). Experiments were performed at least twice with triplicate samples.

with a role of Rac1 in macropinocytosis (Dharmawardhane *et al*, 2000). Nuclear targeting of fluorescent Ad3 was independent of early endosomal antigen 1 (knockdown levels

were larger than 95%; data not shown) and dn caveolin–eGFP (data not shown). Likewise, Ad3 uptake and infection were not affected in cells expressing the dn T27N or

dominant-active Q67L Arf6 mutants (data not shown; Kirkham et al, 2005). The data so far supported the model that crosslinking of CD46 through multiple Ad3 fibres leads to membrane ruffling and macropinosome formation. This process was enhanced by viral engagement with αv integrins and required F-actin, protein kinase C, and Rac1 and gave rise to Ad3-bearing macropinosomal vesicles, some of which had a similar morphological EM appearance as late endosomes and lysosomes. The escape of Ad3 (and the related Ad7) from endosomes approximately 30 min p.i. was considerably slower than the escape of Ad2 ($t_{1/2}$ of 30 min compared to 15 min of Ad2) (Greber et al, 1993), although viral uptake rates were comparable, possibly reflecting different entry pathways of Ad2 and Ad3.

Next, we tested whether the Rac1 target p21-activated kinase 1 (PAK1) was involved in Ad3-stimulated macropinocytosis. PAK1 has been implicated in growth factor-stimulated macropinocytosis in fibroblasts, cell adhesion, and motility (Dharmawardhane et al, 2000; Jaffer and Chernoff, 2002). T423-phospho-PAK1 measurements indicated that Ad3 and Ad5 but not Ad2-ts1 transiently induced PAK1 activation up to 30-fold, although at slightly different rates. Ad3 stimulation peaked at 5–10 min and that of Ad5 at 10–15 min p.i. (Figure 5B). Expression of a PAK1 autoinhibitory domain or two different PAK1 siRNAs (P2, P8) inhibited Ad3 infection and dextran uptake, but not Ad5 infection or transferrin uptake, which were independent of dn PAK1 (Figure 5C and D). Similarly, Ad5 infection was reported to be independent of dominant-active PAK1 in colon cancer SW480 cells (Li et al, 1998). Importantly, the PAK1 siRNAs inhibited the penetration of Ad3 to the cytosol (Figure 5E; data not shown). Collectively, these data suggest a role of PAK1 in Ad3 endocytosis and cytosolic escape but not in endocytosis of Ad5 or transferrin (Meier et al, 2002).

An important effector of activated PAK1 is CtBP1, which is phosphorylated by PAK1 and recruited to the cytoplasm (Barnes et al, 2003). CtBP1 occurs in two splice forms, long and short (CtBP1-L/S). CtBP1-S and CtBP1-L are involved in dynamin-independent endocytosis (Bonazzi et al, 2005). PAK1 phosphorylates CtBP1-L on Ser158 (equivalent to Ser147 of CtBP1-S) within a regulatory domain, disrupts dimers, triggers cytoplasmic localization, and blocks corepressor functions of CtBP1. RNA interference with two different CtBP1 siRNAs (R1, R2) blocked Ad3 but not Ad5 transduction and inhibited fluid-phase uptake in both infected and noninfected cells (Figure 6A–C). R1 had no effects on Ad3 binding, whereas R2 slightly inhibited Ad3 binding to cells (Figure 6D). R1 and R2 inhibited Ad3 endocytosis at both low and high MOI (Figure 6E and F). These results were confirmed by expressing the dn D355A mutant of CtBP1-S, which blocked Ad3 but not Ad5
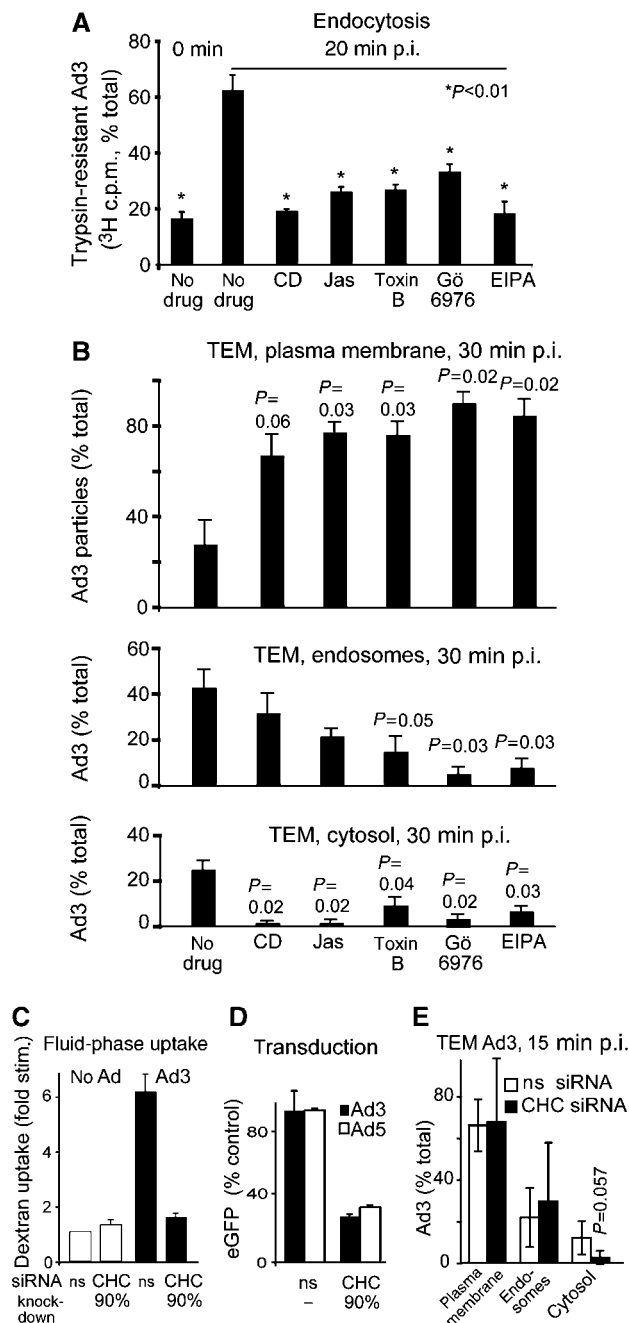


**Figure 4** Ad3 endocytosis and endosomal escape require F-actin, Rho GTPases, PKC, the sodium–proton exchanger 1, and clathrin. (**A**) Endocytosis of Ad3 measured by trypsin sensitivity of cell-surface-localized virus. HeLa-ATCC cells were pretreated with cytochalasin D (CD, 5 μM), jasplakinolide (Jas, 0.3 μM), *Clostridium difficile* toxin B (toxB, 0.3 μg/ml) (Aktories, 1997), Gö6976 (1 μM), or EIPA (100 μM) in growth medium for 30 min, incubated with [³H]thymidine-labelled Ad3 (50 000 c.p.m.) in the cold for 1 h, washed and internalized at 37°C for 20 min, washed with cold medium, and treated with trypsin (2 mg/ml) at 4°C for 1 h. Cells were pelleted by centrifugation at 500 g and the supernatants and cell pellets were analysed by liquid scintillation counting (fraction of total, 100% equivalent to 2000 c.p.m.). (**B**) Analysis of subcellular localization of Ad3 particles by transmission EM. HeLa cells were pretreated with drugs as described in panel A, incubated with Ad3 (30 μg/ml) in the cold, washed with binding medium, internalized in drug-containing medium for 30 min, and fixed for ultra-thin-section EM analyses. Viral particles were quantified at the plasma membrane, in endosomes, and in the cytosol as described (Meier et al, 2005). The total number of particles blindly analysed for each condition was 200–300 in 6–9 different cells. For representative images, see Supplementary Figure 2. (**C–E**) Ad3-stimulated dextran uptake and infection required CHC. Uptake measurements of dextran–FITC in normal HeLa-ATCC cells or cells transfected with nonsilencing siRNA (ns) or siRNA against CHC (CHC, double transfection, 72 h), eGFP transduction measurements, as well as EM analyses were performed as described.
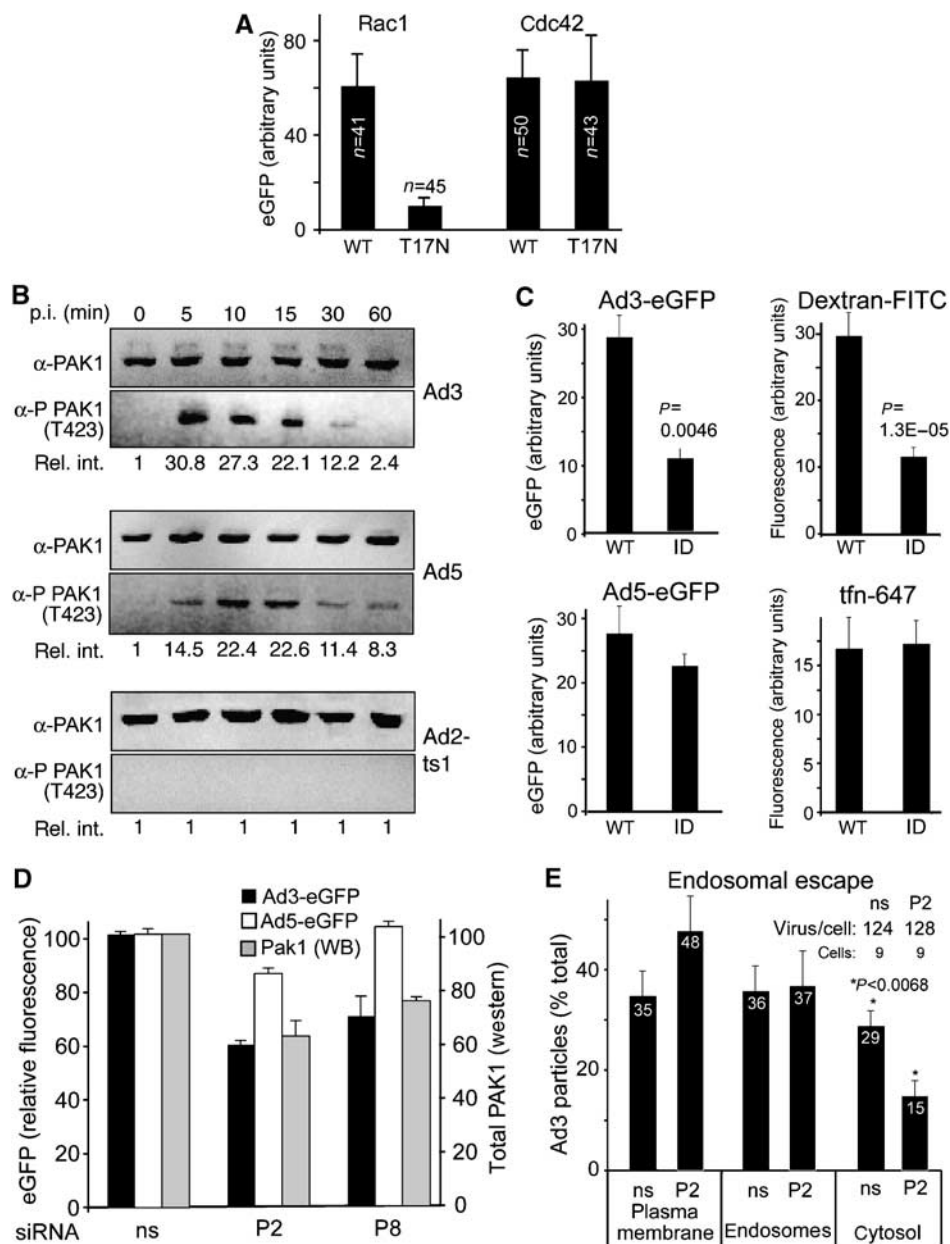
**Figure 5** Rac1 and PAK1 are required for Ad3 but not Ad5 endocytosis and infection. (**A**) HeLa-ATCC cells were transfected with plasmids encoding CFP–Rac1, CFP–Rac1 T17N, CFP–Cdc42, or CFP–Cdc42 T17N for 30 h, infected with Ad3-eGFP for 15 h, fixed, and analysed by confocal laser scanning microscopy. The eGFP intensity of at least 40 CFP-positive cells per condition was quantified by NIH image J with means and standard errors of the mean. The experiment was performed twice with similar results. Representative images are shown in Supplementary Figure 4. (**B**) PAK1 is activated by Ad3 and Ad5. Nonstarved HeLa-ATCC cells were incubated with Ad3, Ad5, or ts1 in the cold, washed, warmed for different times, and analysed for PAK1 and phosphorylated PAK1 (T423) using western blotting. One of three representative experiments is shown including the relative intensities of quantified phospho-PAK1 (rel. int.). (**C**) Cells expressing WT or dn PAK1 (inhibitory domain ID) were transduced with Ad3-eGFP or Ad5-eGFP and assessed for uptake of dextran–FITC or transferrin–Alexa647 upon Ad3 infection. (**D**) Cells were transfected with siRNAs P2 and P8 against PAK1 or nonsilencing (ns) siRNA for 72 h (double transfection, 20 pmol/ml siRNA), infected with Ad3-eGFP or Ad5-eGFP for 6 h, and analysed for eGFP expression by flow cytometry. Transfected cells ($1 \times 10^5$) were analysed by western blotting (WB) for PAK1 (grey panels). (**E**) Endosomal escape of Ad3 measured by thin-section EM in HeLa cells transfected with anti-PAK1 siRNA P2 and ns siRNA. Virions were counted at the plasma membrane, in endosomes, and in the cytosol.

transduction and fluid phase but not transferrin endocytosis, indicating a direct role of CtBP1 in infectious Ad3 endocytosis (Figure 6G). The expression of the phospho-acceptor-defective mutant S147A CtBP1-S but not the phospho-mimetic mutant S147D strongly inhibited Ad3 transduction, supporting a role of phosphorylated S147 in the Ad3 infection cascade. Importantly, S147A CtBP1 had no effect on Ad5-eGFP, indicating that it interfered with an Ad3-specific

process, that is, infectious Ad3 macropinocytosis. The role of CtBP1 and PAK1 in Ad3 infection was independent of the epithelial cell type, as shown by siRNA knockdown in human lung epithelial A549 cells (Figure 6H). As in HeLa cells, Ad5 but not Ad3 transduction of A549 cells was sensitive to dyn2 siRNA. A knockdown of CHC by 78% was, however, not sufficient to inhibit Ad5 or Ad3 infection by more than 20% (data not shown).
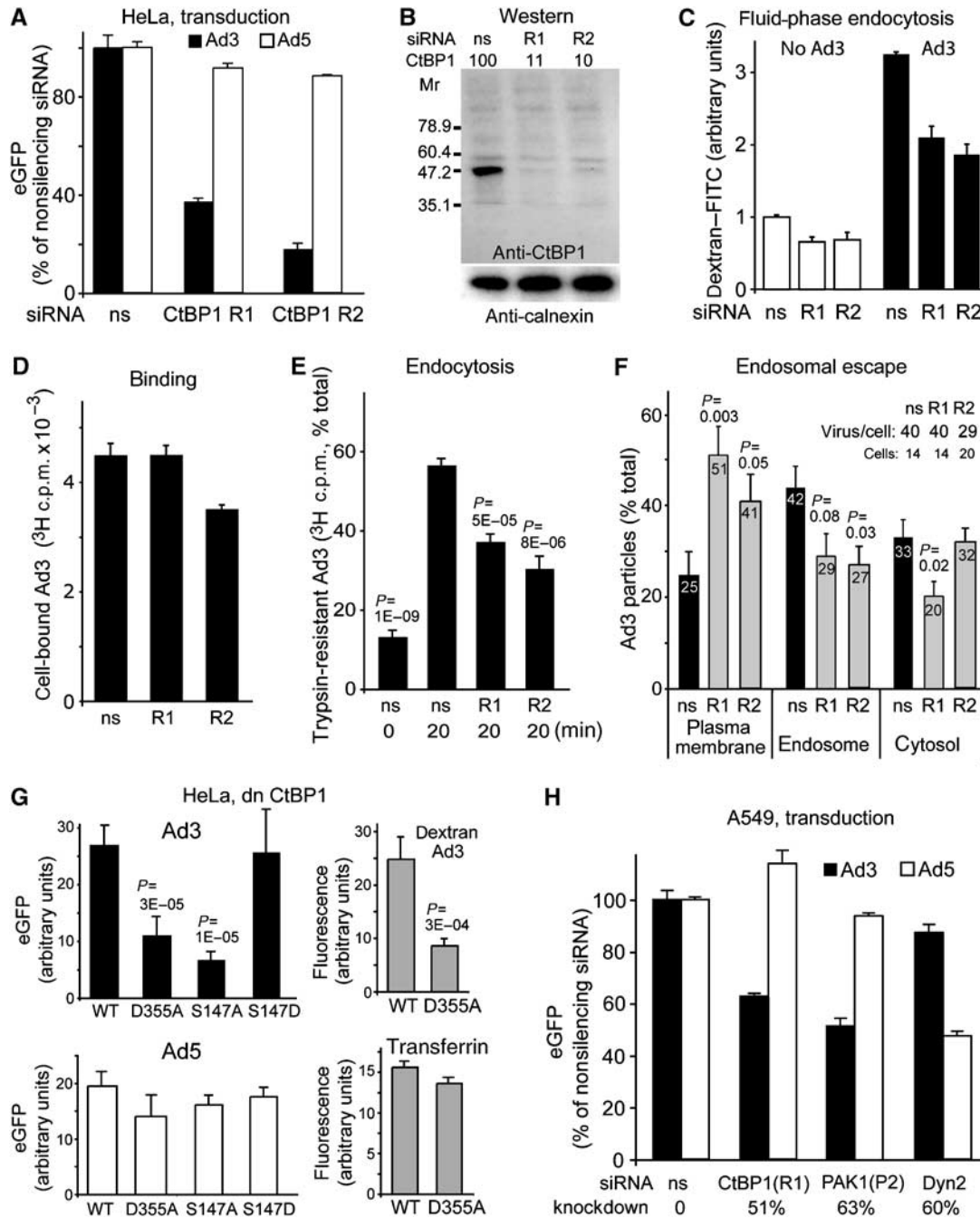
**Figure 6** CtBP1 is required for endosomal uptake and infection of Ad3 but not Ad5. (**A**) HeLa-ATCC cells transfected with CtBP1 siRNA R1 or R2 were infected with Ad3-eGFP or Ad5-eGFP and analysed for GFP expression by flow cytometry. (**B**) Western blot analysis of CtBP1 knockdown by siRNA R1 and R2, or ns siRNA, and normalization against calnexin. (**C**) Fluid-phase endocytosis of HeLa cells transfected with R1, R2, or ns siRNA. Cells were infected with Ad3 or not infected by cold binding and warming for 10 min in the presence of dextran–FITC, fixed, and analysed for dextran uptake by flow cytometry (10 000 cells in triplicate). (**D–F**) Binding and endocytosis of [³H]thymidine-labelled Ad3 were determined by scintillation counting (10⁶ cells, 0.75 μg Ad3) and endosomal escape of Ad3 was determined by EM in cells transfected with anti-CtBP1 siRNA R1, R2, or nonsilencing siRNA. (**G**) HeLa cells were transfected with myc-tagged CtBP1-S WT, CtBP1-S D355A mutant, or the S147A or S147D mutants for 30 h, infected with Ad3-eGFP or Ad5-eGFP at MOI 5 for 16 h, fixed, stained with an anti-myc antibody, and analysed for eGFP fluorescence by confocal laser scanning microscopy and NIH image J analysis of merged set of complete optical sections. CtBP1-S WT- or D355A-transfected cells were pulsed with dextran-TR (0.5 mg/ml) or transferrin–Alexa647 (10 μg/ml) for 30 min, fixed, and analysed for dextran and transferrin uptake by confocal microscopy, respectively (grey panels). (**H**) Human lung epithelial A549 cells were transfected with siRNA against CtBP1 (R1), PAK1 (P2), dyn2, or nonsilencing (ns), transduced with Ad3-eGFP or Ad5-eGFP (MOI 2.5), and analysed for GFP expression by flow cytometry. The levels of knockdown were determined by western blotting using calnexin as a reference.

In noninfected HeLa cells, the majority of endogenous CtBP1 was localized to the nucleoplasm (Figure 7A). In Ad3-infected cells, however, a significant amount of CtBP1 was localized diffusely to the cytoplasm 10 min p.i.

Most noticeably, CtBP1 was present on the periphery of Ad3-bearing macropinosomes (Figure 7A, zoomed-in views). The Ad3-induced dextran-positive macropinosomes contained CD46 and αv integrin receptors, supporting the notion
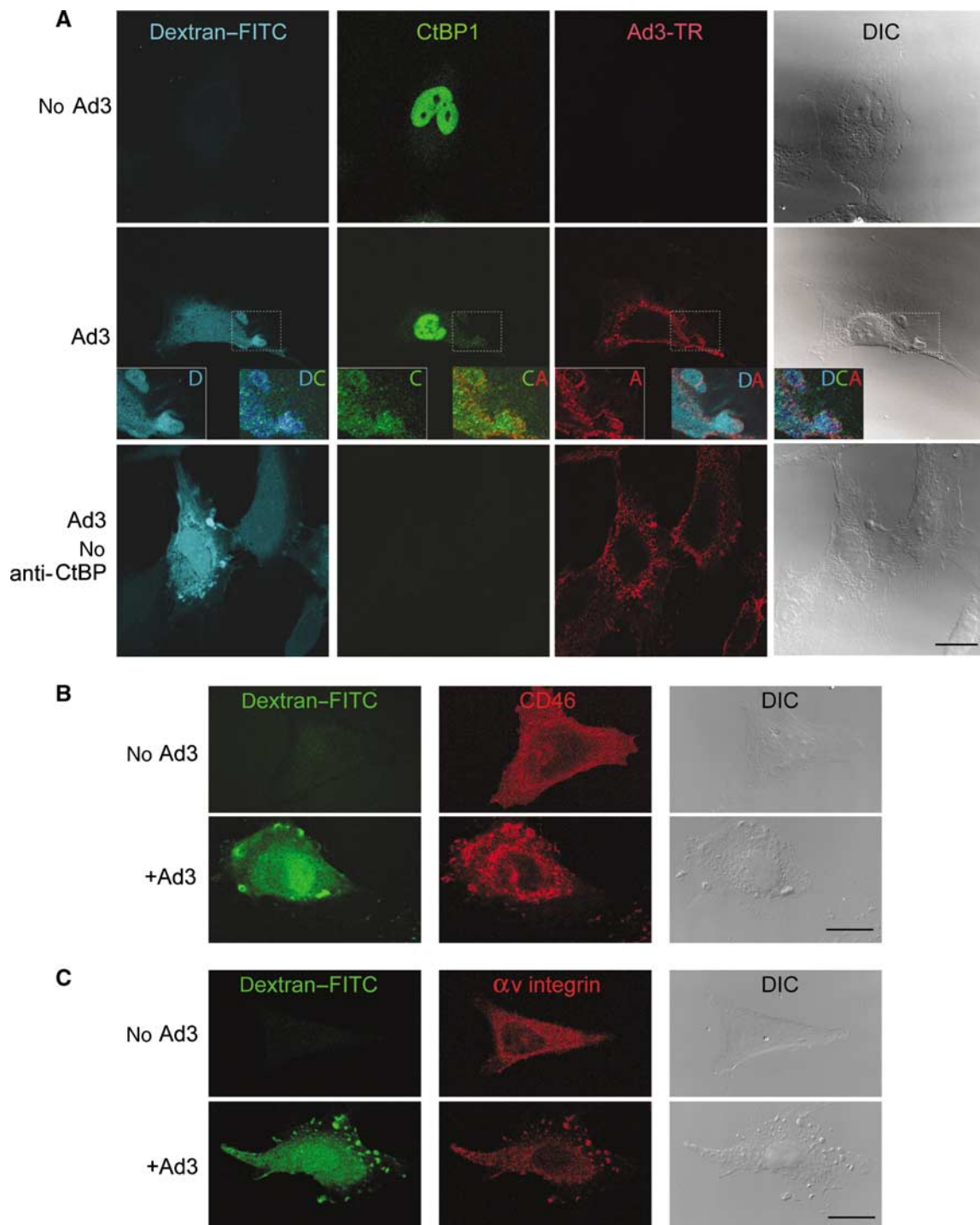
**Figure 7** Ad3-induced macropinosomes contain CtBP1, CD46, and αv β5 integrins. Ad3-TR ($2 \times 10^4$ viral particles/cell, MOI 50)-infected or not infected HeLa-ATCC cells were pulsed with 0.5 mg/ml dextran–FITC at 37°C for 10 min, washed extensively, fixed, immunostained against CtBP1 (0.5 μg/ml), CD46 (mab E4.3, 1 μg/ml), and αv β5 integrins (mab P1F6, 1 μg/ml), and analysed by confocal microscopy (**A–C**). The enlarged boxes in panel A show dextran-filled macropinosomes (D) containing both CtBP1 (C) and Ad3-TR (A). Control stainings in the absence of primary anti-CtBP1 antibody are shown in panel A together with the differential interference contrast images (DIC). Scale bars = 20 μm.

that these vesicles are important for Ad3 infection (Figure 7B). Noninfected cells contained no detectable pinosomes positive for CD46 or integrin. Together, these data support a role of the membrane organizer CtBP1 in the fission or stabilization of Ad3, CD46, and integrin-containing macropinosomal invaginations and vesicles.

### Ad3 infection of haematopoietic cells requires CtBP1 but not clathrin

Human adenoviruses targeting the CD46 receptor have a tropism for haematopoietic cells, unlike the CAR binding adenoviruses. We found that Ad3 induced a robust transient stimulation of dextran uptake in haematopoietic K562 cells
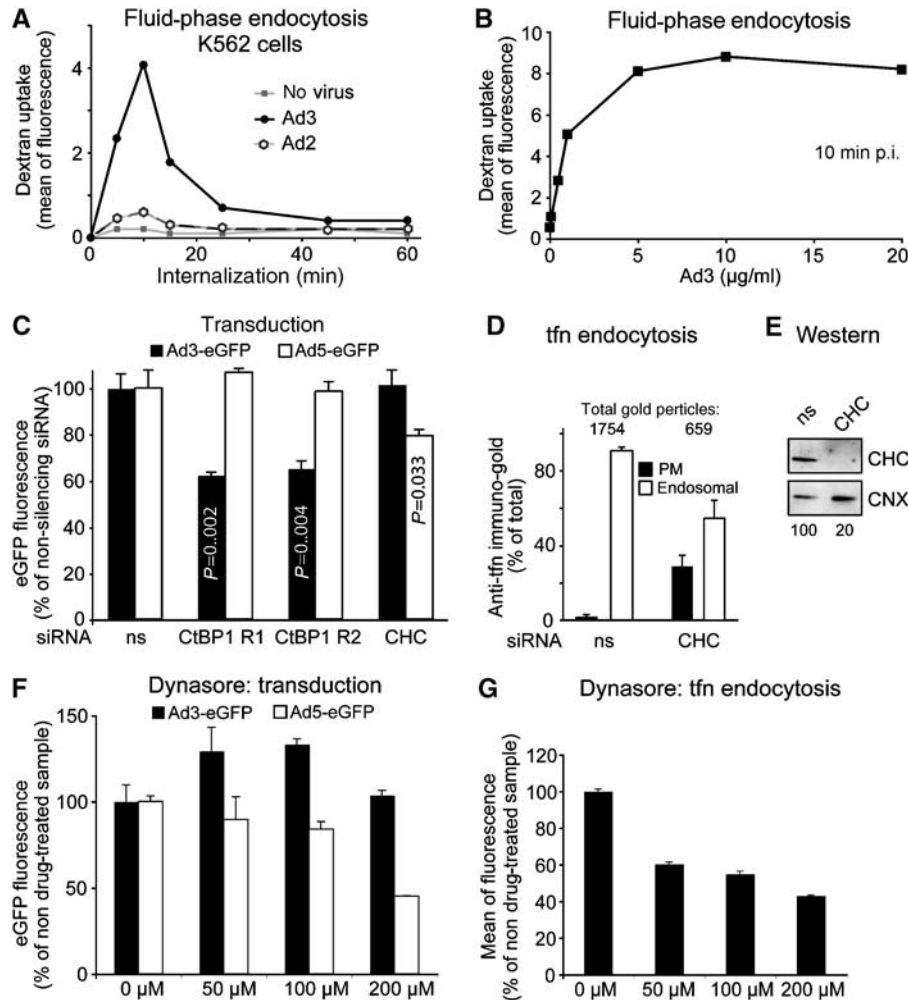
**Figure 8** Infectious Ad3 entry into haematopoietic cells involves fluid-phase endocytosis and CtBP1. (**A**) Haematopoietic K562 cells were infected with Ad3, Ad2 (5 µg/ml virus, equivalent to 2000 viral particles bound per cell), or no virus for different times, pulsed with dextran–FITC (1 mg/ml) for 5 min, and subjected to flow cytometry. (**B**) Dose dependence of fluid-phase uptake stimulation by Ad3 with the indicated amounts of Ad3 in the cold, followed by warming for 5 min and dextran–FITC pulse for 5 min. (**C**) Cells were double transfected with CtBP1 siRNA R1, R2, nonsilencing siRNA (ns), or CHC (CHC) siRNA (20 pmol/ml) for 48 h, infected with Ad3-eGFP (1 µg/ml) or Ad5-eGFP (2 µg/ml) for 16 h, and analysed for eGFP expression by flow cytometry. (**D**) Transferrin (tfn) endocytosis by immuno-EM in CHC siRNA- or control siRNA-treated cells. (**E**) Western blot analyses of CHC siRNA-treated cells ($1 \times 10^5$ cells per lane, normalization against calnexin, CNX). (**F, G**) Dynasore block of Ad3-eGFP (1 µg/ml) or Ad5-eGFP (2 µg/ml) infection for 12 h and transferrin–Alexa488 (10 µg/ml) uptake for 30 min, analysed by flow cytometry.

peaking 10 min p.i. (Figure 8A). In contrast, Ad2 showed a small but significant two-fold stimulation of dextran uptake, for example, reflecting the low levels of CAR in these cells (data not shown). The Ad3-induced dextran stimulation was dose-dependent and saturated at approximately 5 µg/ml virus (about 1000 viral particles bound per cell; Figure 8B). Ad3 transduction of K562 cells was inhibited by CtBP1 siRNAs but not CHC siRNA measured at 16 h p.i. (Figure 8C). In contrast, Ad5 transduction was independent of CtBP1 but sensitive to clathrin siRNA, which blocked transferrin receptor uptake (Figure 8C–E). Further, Ad3 transduction of K562 cells was not affected by the dynamin inhibitor dynasore (Macia *et al*, 2006) up to 200 µM, whereas Ad5-eGFP expression and transferrin uptake were inhibited in a dose-dependent manner (Figure 8F and G). These results underscore a selective requirement of clathrin for macropinocytosis in certain epithelial but not haematopoietic cells and a cell type-independent requirement of CtBP1 for infectious macropinocytosis of Ad3.

## Discussion

Endocytic targeting of human adenoviruses depends on the viral fibre protein and its receptors CAR and CD46, as well as integrin coreceptors, typically αv β5 integrins (Berk, 2007; Stewart and Nemerow, 2007). The data presented here reveal that macropinocytosis is an infectious entry route for the species B human Ad3 in epithelial and haematopoietic cells (Figure 9). The induction of macropinocytosis is, however, not unique to Ad3, but also occurs with Ad2 or Ad5 (Meier *et al*, 2002). Unlike Ad3, Ad2/5 binds CAR and is primarily internalized by dynamin-dependent endocytosis. Ad2/5 infection does not depend on the macropinocytosis regulators CtBP1 and PAK1, unlike Ad3, which utilizes macropinocytosis for infection. Both Ad2/5- and Ad3-induced macropinosomes were CtBP1-positive and they released their fluid contents (data not shown; Meier *et al*, 2002). In addition, macropinocytic stimulation by Ad2/5 and Ad3 involved αv integrins and Rac1. This implies a common
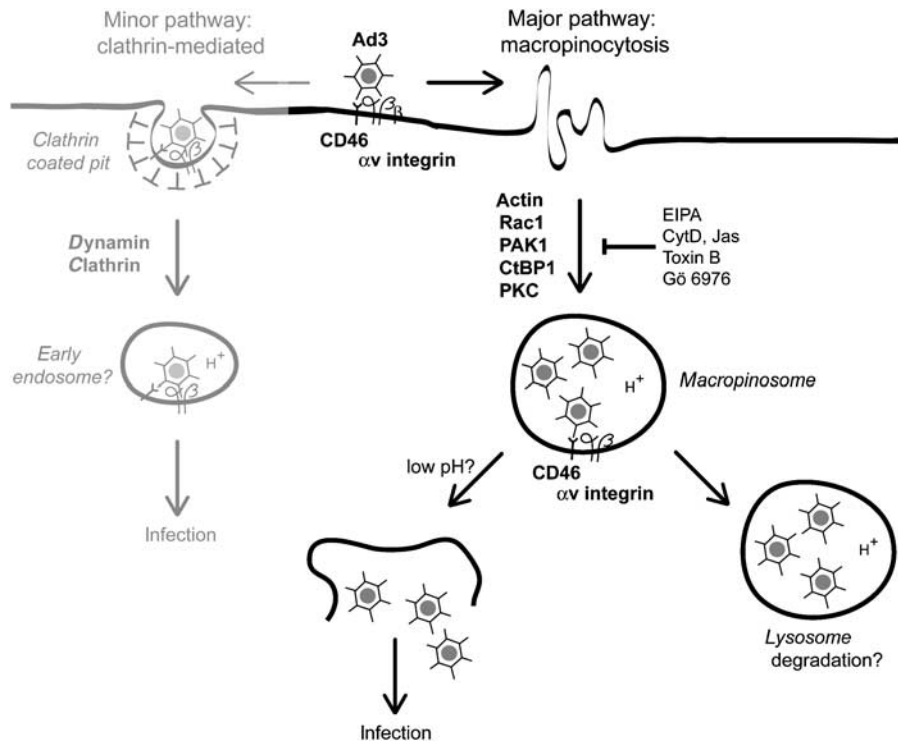
**Figure 9** Macropinocytosis is a major infectious uptake pathway of Ad3 in epithelial cells. Ad3 binds the membrane cofactor CD46 and is endocytosed into macropinocytic vesicles depending on αv β3 or β5 integrin coreceptors, F-actin, the Rac1 GTPase, which activates PAK1, and CtBP1 (C-terminal binding protein 1), a target of PAK1. Protein kinase C (PKC) and the sodium–proton exchanger 1 (sensitive to EIPA) are also required for the formation of Ad3-carrying macropinosomes. Ad3-bearing macropinosomes contain CD46 and αv β5 integrins. Low pH and additional triggers probably lead to virus release from macropinosomes and noninfectious virions are degraded in late endosomes and lysosomes. Besides the major macropinocytic pathway, there is a minor clathrin- and dynamin-dependent pathway, which is cell type-dependent and not found in K562 haematopoietic cells, for example. This pathway remains to be characterized.

mechanism of adenoviral macropinocytosis, which might have been conserved throughout evolution, considering that the hexon sequences of Ad3 and Ad2/5 are as far away from each other as the human Ad hexons from mouse, bovine, or equine hexon sequences (Davison *et al*, 2003).

The stimulation of infectious macropinocytosis by Ad3 required both the CD46 receptor and αv integrin coreceptors. Ligation of both CD46 and αv integrins by antibodies induced fluid-phase uptake, suggesting that CD46 and integrins can provide upstream signals for macropinocytosis. In fact, integrins have been implicated in macropinocytosis and phagocytosis of dead cells (Wu *et al*, 2006). CD46, on the other hand, is a well-known pathogen receptor. It binds vaccine strains of measles virus, human herpes virus 6, the species B human adenoviruses, and bovine viral diarrhoea virus (Cattaneo, 2004). Binding to CD46 may be attractive for pathogens, as CD46 impairs activation and effector function of T cells and their response to NK cells (Oliaro *et al*, 2006). CD46 signalling is also intimately linked to endocytosis. Depending on the degree of ligand crosslinking, CD46 engages in constitutive clathrin-mediated endocytosis, membrane ruffling, or macropinocytosis (Crimeen-Irwin *et al*, 2003). CD46 was, however, not sufficient for Ad3 endocytosis. Infectious Ad3 uptake also required αv integrins. It remains to be determined whether integrins, alone or in conjunction with other cell adhesion molecules, signal macropinocytic uptake in other viral and bacterial infections.

Macropinocytosis has strict requirements for actin, Rac1, protein kinase C, and the sodium/proton exchanger

extruding protons from the cytosol. Proton efflux from the cell through the sodium/proton exchanger is an evolutionarily conserved mechanism for regulating cytoskeleton dynamics, cell migration, growth factor-induced proliferation, and the formation of the phagocytic/macropinocytic cup (Denker and Barber, 2002; Baumgartner *et al*, 2004). It is possible that actin polymerization controlled by Rho GTPases provides the driving force for membrane protrusions and that the actin-anchored sodium–proton exchanger (and perhaps other ion exchangers) contributes to localized volume changes near the plasma membrane. In this scenario, the sodium–proton exchanger would be upstream of Rac1–PAK1–CtBP1 signalling by Ad3. PAK1 activation then triggers CtBP1 translocation to the cytoplasm, which coincides with transcriptional derepression (Barnes *et al*, 2003). The observations that Ad3 but not Ad5 infection was inhibited by dn S147A CtBP3 suggest that Ser147 phosphorylation is important for infectious entry of Ad3. In addition, both Ad3 and Ad2/5 activated PAK1, and CtBP1/3 was found on Ad3- or Ad2/5-induced macropinosomes (the Ad2/5 data are not shown). This suggests that the recruitment of CtBP1 to macropinosomal membranes may contribute to derepression of host genes during Ad2/5 and Ad3 entry.

CtBP family members are important regulators of innate immunity. They bind the immediate-early viral transactivator E1A of all primate and human adenoviruses (Chinnadurai, 2003; Berk, 2005) and regulate the expression of the interferon regulatory factor 3 gene (Johansson *et al*, 2005). Additional CtBP targets include transcriptional coactivators,

such as histone acetyl transferases, and the E1A-associated protein p300 (Chinnadurai, 2002; Senyuk et al, 2005). CD46 and CAR binding adenoviruses induce a strong TLR9-dependent immune response involving NF-κB and various cytokines (Iacobelli-Martinez and Nemerow, 2007). Interestingly, incoming adenoviruses activate protein kinase A, which enhances p300/CBP activity (Mayr and Montminy, 2001; Suomalainen et al, 2001). It is conceivable that PAK1-mediated activation of CtBP1 synergizes with activated TLR9, PKA, and PAK1 to stimulate histone acetylation. This could account for the observation that adenovirus-infected epithelial cells and fibroblasts upregulate a number of CtBP1-repressed genes, such as the CCAAT/enhancer binding protein β, which binds to p300/CBP and CtBP1, and thus could contribute to the establishment of an antiviral state (Schuierer et al, 2001; Zhao et al, 2003; Granberg et al, 2006). We suggest that CtBP1-dependent macropinocytosis is a defence reaction against pathogens that cause transcriptional derepression of innate immunity genes. The ubiquitous nature and high capacity of macropinocytosis in both professional and nonprofessional antigen-presenting cells suggest that it might serve pathogens as an entry gate into different cell types, including polarized epithelial cells (Bruewer et al, 2005). The results presented here may have implications for understanding how endocytic pathogen uptake is connected to the innate immune response in both pathological and therapeutic settings, including gene delivery and vaccination.

## Materials and methods

### Cells and viruses

Cells were grown in DME (GIBCO-BRL) containing 10% FCS (GIBCO-BRL) at low passage number as described (Meier et al, 2002). HeLa-ATCC (CCL-2) cells were purchased from ATCC (American Type Culture Collection), and human melanoma M21 cells (positive for surface-expressed αv integrins) and M21L cells (negative for cell-surface αv integrins) were obtained from Dr D Cheresh (Scripps Research Institute, La Jolla, CA, USA). K562 chronic myelogenous leukaemia cells were grown as described (Meier et al, 2005). Ad3 and Ad2ts1 were grown, labelled with fluorophores, and isolated as described (Suomalainen et al, 2001; Meier et al, 2002). Radiolabelling of virions was carried out as described (Greber et al, 1993). We estimated that 1000 Ad3 particles were equivalent to 2 infectious particles bound per cell (MOI 2), based on a particle to infectious particle ratio of 20, and the observation that 4% of radiolabelled Ad3 bound to cultured human epithelial cells at low MOI (MOI less than 5).

### Ad-eGFP transductions

Cells were washed with warm RPMI–BSA and incubated with 1 μg/ml of Ad3-eGFP (Fleischli et al, 2007) or Ad5-eGFP (Meier et al, 2005) for 60 min, washed several times with RPMI–BSA, and incubated in a water bath for 4 h (A549 cells), 5 h (HeLa cells), 8 h (M21 and M21L cells), and 16 h (K562 cells). The cells were washed with cold PBS and treated with 2% trypsin in the cold, followed by 2% PBS–FCS and analysis by flow cytometry (Beckman FC500 cytometer). At least 10 000 viable cells were counted per sample. For drug experiments, cells were pretreated with inhibitors in RPMI–BSA at 37°C for 30 min, followed by warm infection for 60 min in the presence of drugs followed by washing in medium without drug and further incubation. Data in all experiments are the mean of at least three independent samples with error bars representing standard error of the mean. P-values were calculated using Student's t-tests.

### cDNAs, proteins, and chemicals

K44A-dyn2 and dyn2 WT expression plasmid were from Dr C Lamaze (Pasteur Institute, Paris, France). eGFP-eps15deltaEH2,3 and eGFP-eps15DIIIdelta2 cDNAs were from Dr A Benmerah

(Institut National de la Santé et de la Recherche Médicale E9925, Paris, France; Benmerah et al, 1999) and amphiphysin expression plasmids were from Dr P De Camilli (Yale University, New Haven, USA). Expression plasmids encoding Rac1 WT or dn T17N and Cdc42 WT or dn T17N enhanced by eCFP were from Dr A Hall (University College, London, UK). The Arf6 constructs were obtained from Dr J Donaldson (NIH, Bethesda, MD, USA). cDNAs encoding CtBP1-S were obtained from Dr A Colanzi (Department of Cell Biology and Oncology, S Maria Imbaro, Italy). pCMV-myc CtBP1-S WT was generated by ligation of the PCR-amplified CtBP1-S WT (digested with SalI and NotI) into the pCMV backbone vector (Stratagene). Myc-CtBP1-S D355A was generated using the Quik-ChangeR site-directed mutagenesis kit (Stratagene) with the primers 5'-CTGGGCCAGCATGGCCCCTGCTGTGGTG-3' and 5'-CACCACAG CAGGGGCCATGCTGGCCCAG-3' (Bonazzi et al, 2005). The cDNA was verified by sequencing. PAK1 WT and inhibitory domain expression vectors were from J Chernoff (Fox Chase Cancer Center, Philadelphia, PA, USA). Myc-CtBP1-S S147A was generated with the primers 5'-GAAGGCACTCGGGTCCAGGCTGTAGAGCAGATCCGAGA G-3' and 5'-CTCTCGGATCTGCTCTACAGCCTGGACCCGAGTGCCTT C-3', and myc–CtBP1-S S147D with 5'-GAAGGCACTCGGGTCCAG GATGTAGAGCAGATCCGAGAG-3' and 5'-CTCTCGGATCTGCTCTACA TCCTGGACCCGAGTGCCTTC-3' primers (QuikChangeR site-directed mutagenesis kit, Stratagene). All cDNAs were sequence verified. Toxin B (0.5 mg/ml) and Ad3 soluble fibre knob (final concentration 5 μg/ml) were used as described (Meier et al, 2002; Sirena et al, 2004). Antibodies were from the following sources: anti-CtBP1 (BD-Transduction Laboratories, Switzerland), anti-PAK1 (C-19, Santa Cruz Biotechnology, Santa Cruz, CA, USA), anti-T423 phosphorylated PAK1 (Cell Signaling Technology, Danvers, MA, USA, used as suggested by the manufacturer), anti-calnexin (Ari Helenius, ETH Zürich, Switzerland), anti-CD46 E4.3 (monoclonal, BD-Pharmingen), anti-CD46 (polyclonal H-294, Santa Cruz), anti-αv β5 integrin (P1F6, monoclonal, Chemicon), and secondary rabbit anti-mouse antibody (Pierce). The PKC inhibitor Gö6976 (1 μM) was purchased from Calbiochem (Juro Supply), the Na$^+$/H$^+$ exchanger inhibitor EIPA (100 μM) was from Alexis Corporation, and cytochalasin D (5 μM) and jasplakinolide (500 nM) were from Calbiochem. Dynasore was kindly synthesized by Dr Jay Siegel (Institute of Organic Chemistry, University of Zurich, Switzerland). Cells were pretreated with inhibitors in RPMI–BSA at 37°C for 30 min, infected for 60 min in the presence of drugs followed by washing in medium without drug and further incubations as indicated.

### siRNA transfections

K562 cells were transfected with siRNA directed against CHC (AACCUGCGGUCUGGAGUCAAC) (Qiagen; Meier et al, 2005) and against CtBP1 (CCGUCAAGCAGAUGAGACAUU; GGAUAGAGAC CACGCCAGUUU; Dharmacon; Bonazzi et al, 2005) using Nucleofector I (Amaxa; program T-03) and nonsilencing siRNAs (Qiagen or Dharmacon) as controls. Cells were transfected at days 0 and 2 and analysed at day 4. HeLa cells were transfected with siRNA directed against CHC (Hinrichsen et al, 2003) and CtBP1/CtBP3 or PAK1 (validated siRNA cat. nos. SI00605703 and SI00605696; Qiagen) using Lipofectamine 2000 (Invitrogen) according to the manufacturer's instructions. Cells were transfected twice at days 0 and 2 and analysed at day 4. A549 cells were transfected with dyn2 siRNA (GACAUGAUCCUGCAGUUCA; Qiagen) using Lipofectamine 2000.

### Endocytosis assays

Endocytosis of [$^3$H]thymidine-labelled Ad3 was performed as described (Suomalainen et al, 2001). Transferrin endocytosis was determined by binding a mouse monoclonal anti-transferrin receptor antibody (Thomas Ebel, Karolinska Institute, Huddinge, Sweden) in the cold for 30 min, followed by a secondary anti-mouse antibody coupled to 10 nm gold particles as described (Meier et al, 2005). Antibody–receptor complexes were internalized at 37°C for 30 min and quantified for plasma membrane or endosomal localization of gold particles in a total of five different cells for each condition.

For fluid-phase dextran uptake, cells were preincubated with 5 μg/ml Ad3 in the cold, washed with warm RPMI–BSA, and warmed in RPMI–BSA containing 0.5 mg/ml dextran–FITC (lysine-fixable 10 kDa; Molecular Probes) at 37°C for 10 min, as described earlier (Meier et al, 2002). Dextran uptake was stopped by washing cells with cold RPMI–BSA and PBS (three repeats). Surface-bound

dextran was removed by acid treatment in cold 0.1 M sodium acetate pH 5.5 and 0.05 M NaCl for 10 min. For FACS analysis, cells were detached with 2% trypsin in PBS (GIBCO-BRL) on ice for 25 min, transferred into 6 ml polypropylene tubes (no. 2063; Falcon, Becton Dickinson) containing 2 ml of 7% FCS/PBS, pelleted at 290 g, and resuspended in 2% FCS/PBS. At least 10 000 viable cells were counted per sample in a flow cytometer (Beckman FC500 cytometer). For dextran and transferrin uptake, transfected cells were incubated with 5 µg/ml of Ad3 in the cold, washed, warmed, and then pulsed with a mixture of 0.5 mg/ml dextran-TR and 10 µg/ml transferrin–Alexa647 in RPMI–BSA at 37°C for 30 min (water bath), followed by a 5 min chase. Then they were fixed and mounted for fluorescence analyses (for details see Supplementary data). For antibody-stimulated fluid-phase uptake, primary mouse monoclonal antibodies were incubated with HeLa-ATCC cells in RPMI–BSA on ice for 30 min, washed three times, and then incubated with secondary anti-mouse antibody on ice for 30 min. Cells were warmed up by two quick washes in warm RPMI–BSA, followed by dextran–FITC (0.5 mg/ml) in RPMI–BSA for 10 min, washed, fixed and analysed by flow cytometry. EM and confocal fluorescence microscopy analyses carried out as described (Nakano et al, 2000; Meier et al, 2002). For details, see Supplementary data.

### PAK1 activation and western blots
For PAK1 activation, $5 \times 10^5$ HeLa cells were incubated with 0.5 µg/ml of Ad3, Ad5, or ts1, washed, internalized, chilled with cold PBS containing phosphatase and protease inhibitors, scraped off the dish, resuspended in 100 µl of PBS with inhibitors, mixed with SDS sample buffer, and heated for 30 s. Extracts were separated on 10% SDS–PAGE, transferred to Hybond-ECL nitrocellulose membrane (Amersham Biosciences, Zurich, Switzerland), and blocked with 5% dried milk in 50 mM Tris/100 mM sodium chloride/0.1% Tween, pH 7.4 (TNT). After immunological probing (with 3% milk for the PAK1 blots, with 0.2% BSA for the CtBP1 blots), HRP-conjugated antibodies were detected with ECL-Plus reagents (Amersham Biosciences). Filters were stripped with 100 mM β-mercaptoethanol, 2% SDS, and 62.5 mM Tris/HCl, pH 6.7, at 50°C for 30 min, washed extensively with TNT, blocked with 5% dried milk, and reprobed with a control antibody.

# References

Aktories K (1997) Rho proteins: targets for bacterial toxins. *Trends Microbiol* **5:** 282–288

Barnes CJ, Vadlamudi RK, Mishra SK, Jacobson RH, Li F, Kumar R (2003) Functional inactivation of a transcriptional corepressor by a signaling kinase. *Nat Struct Biol* **10:** 622–628

Baumgartner M, Patel H, Barber DL (2004) Na( + )/H( + ) exchanger NHE1 as plasma membrane scaffold in the assembly of signaling complexes. *Am J Physiol Cell Physiol* **287:** C844–C850

Benmerah A, Bayrou M, Cerf-Bensussan N, Dautry-Varsat A (1999) Inhibition of clathrin-coated pit assembly by an Eps15 mutant. *J Cell Sci* **112:** 1303–1311

Berk AJ (2005) Recent lessons in gene expression, cell cycle control, and cell biology from adenovirus. *Oncogene* **24:** 7673–7685

Berk AJ (2007) Adenoviridae: the viruses and their replication. In: *Fields Virology*, Knipe DM, Howley PM (eds), Vol. 2, pp 2355–2436. Philadelphia, PA, USA: Lippincott Williams & Wilkins

Bonazzi M, Spano S, Turacchio G, Cericola C, Valente C, Colanzi A, Kweon HS, Hsu VW, Polishchuck EV, Polishchuck RS, Sallese M, Pulvirenti T, Corda D, Luini A (2005) CtBP3/BARS drives membrane fission in dynamin-independent transport pathways. *Nat Cell Biol* **7:** 570–580

Bruewer M, Utech M, Ivanov AI, Hopkins AM, Parkos CA, Nusrat A (2005) Interferon-gamma induces internalization of epithelial tight junction proteins via a macropinocytosis-like process. *FASEB J* **19:** 923–933

Cattaneo R (2004) Four viruses, two bacteria, and one receptor: membrane cofactor protein (CD46) as pathogens' magnet. *J Virol* **78:** 4385–4388

Chinnadurai G (2002) CtBP, an unconventional transcriptional corepressor in development and oncogenesis. *Mol Cell* **9:** 213–224

Chinnadurai G (2003) CtBP family proteins: more than transcriptional corepressors. *BioEssays* **25:** 9–12

Colanzi A, Carcedo CH, Persico A, Cericola C, Turacchio G, Bonazzi M, Luini A, Corda D (2007) The Golgi mitotic checkpoint is controlled by BARS-dependent fission of the Golgi ribbon into separate stacks in G2. *EMBO J* **26:** 2465–2476

Crimeen-Irwin B, Ellis S, Christiansen D, Ludford-Menting MJ, Milland J, Lanteri M, Loveland BE, Gerlier D, Russell SM (2003) Ligand binding determines whether CD46 is internalized by clathrin-coated pits or macropinocytosis. *J Biol Chem* **278:** 46927–46937

Damke H, Baba T, Warnock DE, Schmid SL (1994) Induction of mutant dynamin specifically blocks endocytic coated vesicle formation. *J Cell Biol* **127:** 915–934

Davies SP, Reddy H, Caivano M, Cohen P (2000) Specificity and mechanism of action of some commonly used protein kinase inhibitors. *Biochem J* **351:** 95–105

Davison AJ, Benko M, Harrach B (2003) Genetic content and evolution of adenoviruses. *J Gen Virol* **84:** 2895–2908

Denker SP, Barber DL (2002) Ion transport proteins anchor and regulate the cytoskeleton. *Curr Opin Cell Biol* **14:** 214–220

Dharmawardhane S, Schurmann A, Sells MA, Chernoff J, Schmid SL, Bokoch GM (2000) Regulation of macropinocytosis by p21-activated kinase-1. *Mol Biol Cell* **11:** 3341–3352

Fleischli C, Sirena D, Lesage G, Havenga MJ, Cattaneo R, Greber UF, Hemmi S (2007) Species B adenovirus serotypes 3, 7, 11 and 35 share similar binding sites on the membrane cofactor protein CD46 receptor. *J Gen Virol* **88:** 2925–2934

Gallop JL, Butler PJ, McMahon HT (2005) Endophilin and CtBP/BARS are not acyl transferases in endocytosis or Golgi fission. *Nature* **438:** 675–678

Granberg F, Svensson C, Pettersson U, Zhao H (2006) Adenovirus-induced alterations in host cell gene expression prior to the onset of viral gene expression. *Virology* **353:** 1–5

Greber UF, Willetts M, Webster P, Helenius A (1993) Stepwise dismantling of adenovirus 2 during entry into cells. *Cell* **75:** 477–486

Gruenberg J, van der Goot FG (2006) Mechanisms of pathogen entry through the endosomal compartments. *Nat Rev Mol Cell Biol* **7:** 495–504

Gschwendt M, Dieterich S, Rennecke J, Kittstein W, Mueller HJ, Johannes FJ (1996) Inhibition of protein kinase C mu by various inhibitors. Differentiation from protein kinase C isoenzymes. *FEBS Lett* **392:** 77–80

Hayashi S, Hogg JC (2007) Adenovirus infections and lung disease. *Curr Opin Pharmacol* **7:** 237–243

Hinrichsen L, Harborth J, Andrees L, Weber K, Ungewickell EJ (2003) Effect of clathrin heavy chain- and alpha-adaptin-specific small inhibitory RNAs on endocytic accessory proteins and receptor trafficking in HeLa cells. *J Biol Chem* **278:** 45160–45170

Iacobelli-Martinez M, Nemerow GR (2007) Preferential activation of Toll-like receptor nine by CD46-utilizing adenoviruses. *J Virol* **81:** 1305–1312

Jaffer ZM, Chernoff J (2002) p21-activated kinases: three more join the Pak. *Int J Biochem Cell Biol* **34:** 713–717

Johansson C, Zhao H, Bajak E, Granberg F, Pettersson U, Svensson C (2005) Impact of the interaction between adenovirus E1A and CtBP on host cell gene expression. *Virus Res* **113:** 51–63

Kemper C, Verbsky JW, Price JD, Atkinson JP (2005) T-cell stimulation and regulation: with complements from CD46. *Immunol Res* **32:** 31–43

Kirkham M, Fujita A, Chadda R, Nixon SJ, Kurzchalia TV, Sharma DK, Pagano RE, Hancock JF, Mayor S, Parton RG (2005) Ultrastructural identification of uncoated caveolin-independent early endocytic vehicles. *J Cell Biol* **168:** 465–476

Li E, Stupack D, Bokoch GM, Nemerow GR (1998) Adenovirus endocytosis requires actin cytoskeleton reorganization mediated by Rho family GTPases. *J Virol* **72:** 8806–8812

Liszewski MK, Atkinson JP (1996) Membrane cofactor protein (MCP; CD46). Isoforms differ in protection against the classical pathway of complement. *J Immunol* **156:** 4415–4421

Liu NQ, Lossinsky AS, Popik W, Li X, Gujuluva C, Kriederman B, Roberts J, Pushkarsky T, Bukrinsky M, Witte M, Weinand M, Fiala M (2002) Human immunodeficiency virus type 1 enters brain microvascular endothelia by macropinocytosis dependent on lipid rafts and the mitogen-activated protein kinase signaling pathway. *J Virol* **76:** 6689–6700

Macia E, Ehrlich M, Massol R, Boucrot E, Brunner C, Kirchhausen T (2006) Dynasore, a cell-permeable inhibitor of dynamin. *Dev Cell* **10:** 839–850

Marechal V, Prevost MC, Petit C, Perret E, Heard JM, Schwartz O (2001) Human immunodeficiency virus type 1 entry into macrophages mediated by macropinocytosis. *J Virol* **75:** 11166–11177

Marsh M, Helenius A (2006) Virus entry: open sesame. *Cell* **124:** 729–740

Marttila M, Persson D, Gustafsson D, Liszewski MK, Atkinson JP, Wadell G, Arnberg N (2005) CD46 is a cellular receptor for all species B adenoviruses except types 3 and 7. *J Virol* **79:** 14429–14436

Mathias P, Wickham T, Moore M, Nemerow G (1994) Multiple adenovirus serotypes use alpha-v integrins for infection. *J Virol* **68:** 6811–6814

Mayor S, Pagano RE (2007) Pathways of clathrin-independent endocytosis. *Nat Rev Mol Cell Biol* **8:** 603–612

Mayr B, Montminy M (2001) Transcriptional regulation by the phosphorylation-dependent factor creb. *Nat Rev Mol Cell Biol* **2:** 599–609

Meier O, Boucke K, Vig S, Keller S, Stidwill RP, Hemmi S, Greber UF (2002) Adenovirus triggers macropinocytosis and endosomal leakage together with its clathrin mediated uptake. *J Cell Biol* **158:** 1119–1131

Meier O, Gastaldelli M, Boucke K, Hemmi S, Greber UF (2005) Early steps of clathrin-mediated endocytosis involved in phagosomal escape of Fc-g receptor targeted adenovirus. *J Virol* **79:** 2604–2613

Miyazawa N, Leopold PL, Hackett NR, Ferris B, Worgall S, Falck-Pedersen E, Crystal RG (1999) Fiber swap between adenovirus subgroups B and C alters intracellular trafficking of adenovirus gene transfer vectors. *J Virol* **73:** 6056–6065

Nakano MY, Greber UF (2000) Quantitative microscopy of fluorescent adenovirus entry. *J Struct Biol* **129:** 57–68

Nakano MY, Boucke K, Suomalainen M, Stidwill RP, Greber UF (2000) The first step of adenovirus type 2 disassembly occurs at the cell surface, independently of endocytosis and escape to the cytosol. *J Virol* **74:** 7085–7095

Oliaro J, Pasam A, Waterhouse NJ, Browne KA, Ludford-Menting MJ, Trapani JA, Russell SM (2006) Ligation of the cell surface receptor, CD46, alters T cell polarity and response to antigen presentation. *Proc Natl Acad Sci USA* **103:** 18685–18690

Orth JD, Krueger EW, Weller SG, McNiven MA (2006) A novel endocytic mechanism of epidermal growth factor receptor sequestration and internalization. *Cancer Res* **66:** 3603–3610

Owen DJ, Wigge P, Vallis Y, Moore JD, Evans PR, McMahon HT (1998) Crystal structure of the amphiphysin-2 SH3 domain and its role in the prevention of dynamin ring formation. *EMBO J* **17:** 5273–5285

Persson BD, Reiter DM, Marttila M, Mei YF, Casasnovas JM, Arnberg N, Stehle T (2007) Adenovirus type 11 binding alters the conformation of its receptor CD46. *Nat Struct Mol Biol* **14:** 164–166

Popoff V, Mardones GA, Tenza D, Rojas R, Lamaze C, Bonifacino JS, Raposo G, Johannes L (2007) The retromer complex and clathrin define an early endosomal retrograde exit site. *J Cell Sci* **120:** 2022–2031

Riley-Vargas RC, Gill DB, Kemper C, Liszewski MK, Atkinson JP (2004) CD46: expanding beyond complement regulation. *Trends Immunol* **25:** 496–503

Schnatwinkel C, Christoforidis S, Lindsay MR, Uttenweiler-Joseph S, Wilm M, Parton RG, Zerial M (2004) The Rab5 effector Rabankyrin-5 regulates and coordinates different endocytic mechanisms. *PLoS Biol* **2:** E261

Schuierer M, Hilger-Eversheim K, Dobner T, Bosserhoff AK, Moser M, Turner J, Crossley M, Buettner R (2001) Induction of AP-2alpha expression by adenoviral infection involves inactivation of the AP-2rep transcriptional corepressor CtBP1. *J Biol Chem* **276:** 27944–27949

Senyuk V, Sinha KK, Nucifora G (2005) Corepressor CtBP1 interacts with and specifically inhibits CBP activity. *Arch Biochem Biophys* **441:** 168–173

Sirena D, Lilienfeld B, Eisenhut M, Kaelin S, Boucke K, Beerli RR, Vogt L, Ruedl C, Bachmann MF, Greber UF, Hemmi S (2004) The human membrane cofactor CD46 is a receptor for species B adenovirus serotype 3. *J Virol* **78:** 4454–4462

Stewart PL, Nemerow GR (2007) Cell integrins: commonly used receptors for diverse viral pathogens. *Trends Microbiol* **15:** 500–507

Suomalainen M, Nakano MY, Boucke K, Keller S, Greber UF (2001) Adenovirus-activated PKA and p38/MAPK pathways boost microtubule-mediated nuclear targeting of virus. *EMBO J* **20:** 1310–1319

tom Dieck S, Altrock WD, Kessels MM, Qualmann B, Regus H, Brauner D, Fejtova A, Bracko O, Gundelfinger ED, Brandstatter JH (2005) Molecular dissection of the photoreceptor ribbon synapse: physical interaction of Bassoon and RIBEYE is essential for the assembly of the ribbon complex. *J Cell Biol* **168:** 825–836

Verger A, Quinlan KG, Crofts LA, Spano S, Corda D, Kable EP, Braet F, Crossley M (2006) Mechanisms directing the nuclear localization of the CtBP family proteins. *Mol Cell Biol* **26:** 4882–4894

Wu Y, Tibrewal N, Birge RB (2006) Phosphatidylserine recognition by phagocytes: a view to a kill. *Trends Cell Biol* **16:** 189–197

Zhao H, Granberg F, Elfineh L, Pettersson U, Svensson C (2003) Strategic attack on host cell gene expression during adenovirus infection. *J Virol* **77:** 11006–11015